LIN-5 Is a Novel Component of the Spindle Apparatus Required for Chromosome Segregation and Cleavage Plane Specification in *Caenorhabditis elegans*

Monique A. Lorson,* H. Robert Horvitz,‡ and Sander van den Heuvel*‡

*Massachusetts General Hospital Cancer Center, Charlestown, Massachusetts 02129; and ‡Howard Hughes Medical Institute, Department of Biology, Massachusetts Institute of Technology, Cambridge, Massachusetts 02139

Abstract. Successful divisions of eukaryotic cells require accurate and coordinated cycles of DNA replication, spindle formation, chromosome segregation, and cytoplasmic cleavage. The *Caenorhabditis elegans* gene *lin-5* is essential for multiple aspects of cell division. Cells in *lin-5* null mutants enter mitosis at the normal time and form bipolar spindles, but fail chromosome alignment at the metaphase plate, sister chromatid separation, and cytokinesis. Despite these defects, cells exit from mitosis without delay and progress through subsequent rounds of DNA replication, centrosome duplication, and abortive mitoses. In addition, early embryos that lack *lin-5* function show defects in spindle positioning and cleavage plane specification. The *lin-5* gene encodes a novel protein with a central coiled-coil domain. This protein localizes to the spindle apparatus in a cell cycle- and microtubule-dependent manner. The LIN-5 protein is located at the centrosomes throughout mitosis, at the kinetochore microtubules in metaphase cells, and at the spindle during meiosis. Our results show that LIN-5 is a novel component of the spindle apparatus required for chromosome and spindle movements, cytoplasmic cleavage, and correct alternation of the S and M phases of the cell cycle.

Key words: *lin-5* • mitosis • cytokinesis • microtubules • mitotic checkpoint

Introduction

During cell division, many biochemical processes must be accurately executed and well orchestrated to generate daughter cells that are genetically intact (for review, Nasmyth, 1996). First, the DNA should be replicated entirely during S phase of the cell cycle. Next, a bipolar spindle should be formed, attached to all chromosomes, and used to segregate the sister chromatids to opposite poles. Subsequently, the cytoplasm needs to be cleaved between the segregated chromosomes in a plane perpendicular to the spindle. Additionally, the spindle should be positioned correctly before cleavage, to control the direction of division and to determine whether cytoplasmic components are divided in a symmetric or asymmetric manner.

The molecular mechanisms involved in accurate chromosome segregation have been partially elucidated, mostly through genetic studies of yeast, biochemical studies of *Xenopus* and cell biological studies of mammalian tissue-culture cells. Meiotic and mitotic spindles have been shown to consist of microtubules and associated proteins (for review, Desai and Mitchison, 1997). The microtubules assemble by polymerization of αβ-tubulin dimers. Polymerization is usually initiated at microtubule-organizing centers (MTOCs)[1]. Microtubules are polar; they contain minus ends that usually remain associated with the MTOC and plus ends that extend into the cytoplasm and undergo rapid growth and shrinkage. Motor proteins of the dynein and kinesin families use the polarity of these microtubules to generate force in either the plus or minus end direction (for review, Hoyt and Geiser, 1996). The role of the MTOC in spindle formation is still unclear. MTOCs can vary greatly in morphology, as is evident when comparing centrosomes in animal cells and spindle pole bodies in yeast (Stearns and Winey, 1997). In addition, spindles can be formed without centrosomes in certain cell divisions, for instance during female meiosis in many animals

Address correspondence to Sander van den Heuvel, Massachusetts General Hospital Cancer Center, Building 149, 13th Street, Charlestown, MA 02129. Tel.: (617) 726-5605. Fax: (617) 724-9648. E-mail: heuvel@helix.mgh.harvard.edu

[1]*Abbreviations used in this paper:* BrdU, 5-bromo-2'deoxyuridine; Cdk, cyclin-dependent kinase; DAPI, 4,6-diamidino-2-phenylindole; MTOC, microtubule-organizing center; ORF, open reading frame; PI, propidium iodide; RNAi, RNA mediated interference; ts, temperature-sensitive.

© The Rockefeller University Press, 0021-9525/2000/01/73/14 $5.00

(McKim and Hawley, 1995). However, in most cell divisions, the MTOCs duplicate, separate to opposite poles, and form two sites for microtubule nucleation. In this way, MTOCs contribute to the bipolar nature of the spindle, as well as to rapid and directional assembly of microtubules.

The mitotic functions of the spindle apparatus include separation of the centrosomes, segregation of sister chromatids, and specification of the cleavage-plane position. These different tasks depend on correct localization and activation of a large number of microtubule-associated motor proteins. In addition, activity of these motor proteins needs to be coordinated with microtubule assembly and disassembly. Multiple levels of regulation control the timing and execution of these mitotic processes. The cyclin-dependent protein kinase Cdk1/Cdc2 is the key regulator of mitosis in all eukaryotes studied (for reviews, Morgan, 1997; Mendenhall and Hodge, 1998). Activation of Cdk1/Cdc2 in association with a mitotic cyclin is essential for entry into mitosis, whereas exit from mitosis requires inactivation of this kinase and degradation of the cyclins. Phosphorylation of substrates by Cdk1/Cdc2 is thought to induce major events in M phase, such as chromosome condensation, nuclear envelope degradation, and spindle formation. Checkpoint controls can interrupt the periodic activation and inactivation of Cdk's, thereby pausing cell cycle progression and allowing time for the completion of earlier events (for review, Elledge, 1996).

It is likely that components with important roles in the accurate segregation of chromosomes are yet to be identified. In addition, it remains largely unknown how the many molecules involved are temporally and spatially regulated. The nematode *Caenorhabditis elegans* provides an animal model excellently suited for further cell division studies. The transparency of *C. elegans* allows monitoring of cell division and chromosome segregation in living animals. The invariance of the cell lineage has allowed a precise description of the time and plane of division for every somatic cell (Sulston and Horvitz, 1977; Sulston et al., 1983), which provides a unique tool in the identification and characterization of cell cycle mutants. The cloning of genes defined by such mutants is facilitated by powerful genetics (Brenner, 1974) and a completely sequenced genome (*C. elegans* Sequencing Consortium, 1998). In addition, the centrosomes and spindle are similar in structure and function to those in other animal cells and the formation and orientation of the spindle during *C. elegans* embryogenesis have been described in detail (reviewed by Strome, 1993; White and Strome, 1996).

To improve our understanding of the mechanisms involved in accurate chromosome segregation in animal cells, we have characterized the *C. elegans* gene *lin-5*. Cells in homozygous *lin-5* mutants cycle through abortive mitoses, alternated with subsequent rounds of DNA replication (Albertson et al., 1978; Sulston and Horvitz, 1981). We have cloned the *lin-5* gene and found that it encodes a novel protein localized most prominently at the centrosomes during mitosis and at the spindle in meiosis. The defects observed in *lin-5* mutants and the localization of the LIN-5 protein indicate primary functions in chromosome segregation and spindle positioning and potential secondary roles in cytokinesis and coupling the S and M phases.

Materials and Methods

Strains and Genetics

C. elegans strains were derived from the wild-type Bristol strain N2 and Bergerac strain RW7000 and cultured using standard techniques as described by Brenner (1974). We used the following mutations, descriptions of which can be found in Riddle et al. (1997) or this study: LGII, *dpy-10(e128), lin-5(e1348, e1457, n3066, n3070, ev571ts), rol-6(su1006), unc-4(e120), rol-1(e91), mnC1[dpy-10(e128) unc-52(e444)], mnDf100.*

Allele *ev571ts* was kindly provided by David Merz and Joe Culotti (Mt. Sinai Hospital Research Institute, Toronto). Mutations *n3066* and *n3070* were isolated in this study. N2 animals were mutagenized with 50 mM ethyl methanesulfonate (EMS) as described by Brenner (1974). F1 progeny were placed on separate plates and examined for thin, sterile, and uncoordinated F2 self progeny. Mutants that at least partly resembled *lin-5* mutants were examined for defects in cell division and polyploidy, using Nomarski optics or fluorescence microscopy of Carnoy's-fixed 4,6-diamidino-2-phenylindole (DAPI)-stained animals (Wood et al., 1988). Candidate mutations were recovered from siblings and were mapped either with recessive genetic markers or by PCR, making use of primers based on polymorphic sequence-tagged sites in the RW7000 Bergerac strain (Williams et al., 1992). *lin-5* mutations mapped to chromosome II and were localized by standard three-factor crosses (Wood, 1988) between *dpy-10(e128)* and *unc-4(e120)*, or *dpy-10(e128)* and *rol-1(e91)*, ~0.56 map units to the right of *dpy-10*. In addition, all *lin-5* mutations failed to complement *mnDf100* and the *lin-5* allele *e1348*. A genetic characterization of the *lin-5* alleles will be described elsewhere.

Germline Transformation Rescue

Germline transformation experiments were performed as described by Mello et al. (1991). Animals of genotype *lin-5(e1348) unc-4(e120)/mnC1[dpy-10(e128) unc-52(e444)]* were injected with cosmids or plasmids containing *C. elegans* genomic DNA (1–20 μg/ml) and pRF4 (80 μg/ml), which contains the dominant marker *rol-6(su1006)*. Rescue was examined in the F1 self progeny or in the F2 self progeny from animals that displayed the Rol phenotype. The presence of multiple Unc Rol progeny with at least partially formed vulva was scored as rescue. Such animals typically contained a more extensive germ line than *lin-5(e1348)* mutants and several oocytes or embryos, but nearly invariably failed to produce viable progeny. Similar experiments were performed to examine rescue with *lin-5* cDNAs transcriptionally fused to the heat-shock promoters of plasmids pPD48.78 and pPD49.87 and injected at a concentration of 50 μg/ml, together with pRF4 (Fire et al., 1990). After establishing transgenic lines, we shifted embryos to 33°C for 1 h and scored rescue in the adults.

Isolation of lin-5 cDNA

Standard molecular biology protocols were used as described by Sambrook et al. (1989). The genomic sequence of the *lin-5* region was obtained by the *C. elegans* Genome Sequencing Consortium (1998). Subfragments were cloned based on these sequences and open reading frames (ORFs) predicted by GENEFINDER. A 2-kb segment from the minimal rescue fragment was used to screen embryonic and mixed-stage cDNA libraries (Okkema and Fire, 1994), 6×10^6 clones each. DNA sequences were obtained from four of the cDNA inserts, using an automated ABI 373A DNA sequencer (Applied Biosystems). The sequences of mutant alleles were determined from PCR-amplified genomic DNA. All primers were designed based upon the genomic sequences and are available upon request. The coiled-coil domain was predicted using MacStripe, a Macintosh version of the algorithm originally designed by Lupas et al. (1991), and was kindly provided by Alex Knight (University of Cambridge, MA).

RNA Mediated Interference

Plasmids containing full-length *lin-5* cDNA were used for in vitro transcription. Genomic DNA containing part of the F01G10.5 sequence was obtained by PCR amplification with primers 5′-acccagctccatgtgattta and either primer 5′-gggagaatccacaacttc or 5′-tccagctctatccagttg, resulting in fragments of 866 and 1,680 bp, respectively. Sense and antisense transcripts were generated using linearized templates and T3 and T7 RNA polymerases. RNA was extracted with phenol, precipitated with ethanol, and dissolved in TE (10 mM Tris-Cl pH 8.0, 0.1 mM EDTA) to a final

concentration of 1 mg/ml. A 1:1 mixture of the two strands was injected into young adult N2 hermaphrodites as described by Fire et al. (1998).

Antibodies and Immunohistochemistry

A 3′ fragment of the *lin-5* cDNA (1,138 bp SalI–BamHI) was cloned into the pET19b expression vector (Novagen) and expressed in *Escherichia coli*. The purified His-tagged LIN-5 COOH-terminal fragment was injected into mice. Fusion of splenocytes with myeloma Sp2 cells and selection of hybridomas was performed according to standard procedures (Harlow and Lane, 1998). Tissue culture supernatants from three independent LIN-5–reactive clones (hel-1, hel-2, and hel-3) were used in these studies, either individually or as a mixture with equal ratio. Antibodies produced by clones hel-1 and hel-2 are of the IgG1 isotype, whereas hel-3 produced IgG2a heavy chains. All light chains were of the κ-type.

Immunostaining of *C. elegans* embryos was performed as described by Strome and Wood (1983) with minor modifications (Boxem et al., 1999). Immunostaining of larvae was performed according to standard procedures, using synchronously grown animals fixed in paraformaldehyde or Bouin's reagent (Boxem et al., 1999). To visualize DNA synthesis, a solution of 5-bromo-2′deoxyuridine (BrdU, final concentration 0.5 mg/ml; Sigma Chemical Co.) in S-medium was added to staged L1 animals at 6 h of L1 development. Animals were collected 6–8 h later, washed three times in M9, and fixed in Bouin's fixative (Boxem et al., 1999).

The antibodies used in these studies were: tissue culture supernatant of anti–LIN-5 mouse mAbs, 1:2 diluted; rabbit polyclonal serum against phosphorylated histone H3 (Upstate Biotechnology), 1:300 diluted; mouse monoclonal anti-BrdU antibodies (Sigma Chemical Co.), 1:60 diluted; anti–α-tubulin DM1A mouse mAbs (Sigma Chemical Co.), 1:100 diluted; and anti–α-tubulin YOL1/34 and YL1/2 rat mAbs, 1:50 diluted (Harlan Sera-Lab). Secondary FITC-, TRITC-, or Texas red-conjugated antibodies were used at 1:100 dilution (Cappel Research and Jackson ImmunoResearch Laboratories). DNA was stained with either propidium iodide (PI) 1 μg/ml, after treatment with 200 μg/ml RNAse A for 30 min, or with 1 μg/ml DAPI (Sigma Chemical Co.). Samples were mounted on slides in glycerol with 10% PBS and 2.3% Dabco (Sigma Chemical Co.).

Timing of Mitosis and Cdk1/NCC-1 Kinase Activity

Progeny from parents of wild-type, *lin-5(e1348)*/+, or *lin-5(ev571*ts*)* genotype were harvested by hypochlorite treatment and allowed to develop at 15°C to early L1 stage in the absence of food. Larvae were transferred to plates with bacteria and shifted to 20, 23, or 25°C. Synchronously developing animals were examined by microscopy with Nomarski optics, and the time in mitosis recorded for the first (abortive) divisions in the P cell lineages. The duration of mitosis was determined as the time from disappearance of the nucleolus until reformation of the nuclear envelope. For each genotype, ~50 nuclei were scored at 23°C and 20–30 nuclei at 25°C. Cdk1 kinase activity was examined in individual cells using phosphorylation of histone H3 as a reporter for kinase activity. Antibodies raised against a Cdk1-phosphorylated histone H3 peptide recognize a mitotic epitope in several eukaryotes including *C. elegans* (Lieb et al., 1998). This epitope has been shown to disappear upon RNA interference of *ncc-1*, the mitotic Cdk1 kinase in *C. elegans* (Boxem et al., 1999). Synchronized wild-type and *lin-5(e1348)* L1 larvae were fixed and stained 9 h after feeding at 25°C. Cells in the P lineage were scored for histone H3 staining and for mitotic stage, based on DNA condensation and chromosome arrangement.

Determination of Spindle Orientation by Immunostaining and Video Recordings

Spindle orientations were determined in two-cell embryos that were fixed and stained with anti–α-tubulin antibody DM1A and PI. Embryos were obtained by dissecting gravid N2 hermaphrodites, uninjected or *lin-5* dsRNA injected, or *lin-5(ev571)* hermaphrodites shifted to the nonpermissive temperature of 26°C for 9 h. Spindle positions were scored in two-cell embryos with prometaphase to anaphase cells, after the P1 spindle–nucleus complex should have rotated. Spindle orientations were recorded as transverse if the angle of the spindle relative to the long axis of the embryo was >45° or longitudinal if this angle was <45° (Rose and Kemphues, 1998). Spindles were scored as abnormal if the centrosome–nuclear complex was mispositioned within the context of the cell. Early embryonic events were recorded with time-lapse video microscopy, performed on embryos that were dissected from adults or in adult animals anaesthetized with 0.1% tricaine and 0.01% tetramisole as described previously (Kirby et al., 1990).

Nocodazole Treatment

To obtain embryos, gravid hermaphrodites were dissected in M9 buffer containing DMSO (control) or 20 μg/ml nocodazole dissolved in DMSO (Sigma Chemical Co.). Coverslips were placed over the slides, and pressure was applied to permeabilize the eggshell. The slides were incubated in a humid chamber for 15 min at room temperature and then freeze-cracked, fixed, and immunostained as described. Disruption of the microtubules was determined by immunostaining with the anti–α-tubulin antibodies YOL1/34 and YL1/2. *C. elegans* larvae appeared highly resistant to all microtubule-interfering drugs tested, including nocodazole, colchicine, colchemid, vinchristine, and vinblastine, even at concentrations 1,000-fold higher than usually applied to tissue-culture cells.

Microscopy and Image Acquisition

A Zeiss Axioplan II microscope was used for Nomarski differential interference and immunofluorescence microscopy. Confocal images were obtained using a Leica inverted microscope and Leitz imaging software. In addition, images were acquired with a Sensys cooled CCD camera (Photometrics), followed by image analysis and computational deconvolution with Openlabs software (Improvision). Images were pseudocolored and merged using Adobe Photoshop.

Results

lin-5 Is Required for Cell Divisions

The *C. elegans* gene *lin-5* was previously defined by two recessive mutations isolated in screens for cell lineage mutants (Horvitz and Sulston, 1980; Sulston and Horvitz, 1981). Aspects of the mutant phenotype have been described by Albertson et al. (1978). Based on molecular and genetic criteria, the previously isolated *lin-5* alleles, *e1348* and *e1457*, and our newly isolated mutations, *n3066* and *n3070*, are strong loss-of-function or null alleles (see below and data not shown). These mutations cause recessive phenotypes, including complete sterility, and are phenotypically indistinguishable. We have characterized the *e1348* mutation most thoroughly. This mutation appears to eliminate *lin-5* function and is also referred to below as *lin-5(0)*.

Homozygous *lin-5* mutants derived from heterozygous hermaphrodites complete embryonic development, but fail to undergo postembryonic nuclear and cytoplasmic divisions (Albertson et al., 1978; Fig. 1, A and B). Microscopic analyses using Nomarski optics revealed that cells entered mitosis at the normal times during larval development of *lin-5(e1348)* mutants, as manifested by disappearance of the nucleolus, condensation of the chromatin, and degradation of the nuclear envelope (Albertson et al., 1978). Chromosome movements towards the equatorial plane were initiated, but metaphase-plate formation was almost invariably incomplete, anaphase failed to occur, and neither nuclear division nor cell division was initiated (Fig. 2; and data not shown). Despite the lack of chromosome segregation, cells exited from mitosis without significant delay, the chromatin relaxed, and a nuclear envelope reformed (Fig. 3).

We examined phosphorylation of a histone H3 epitope to assay activity of the mitotic kinase NCC-1(Cdk1) (see Materials and Methods). Synchronously developing wild-type and *lin-5(e1348)* L1 larvae were found to contain sim-

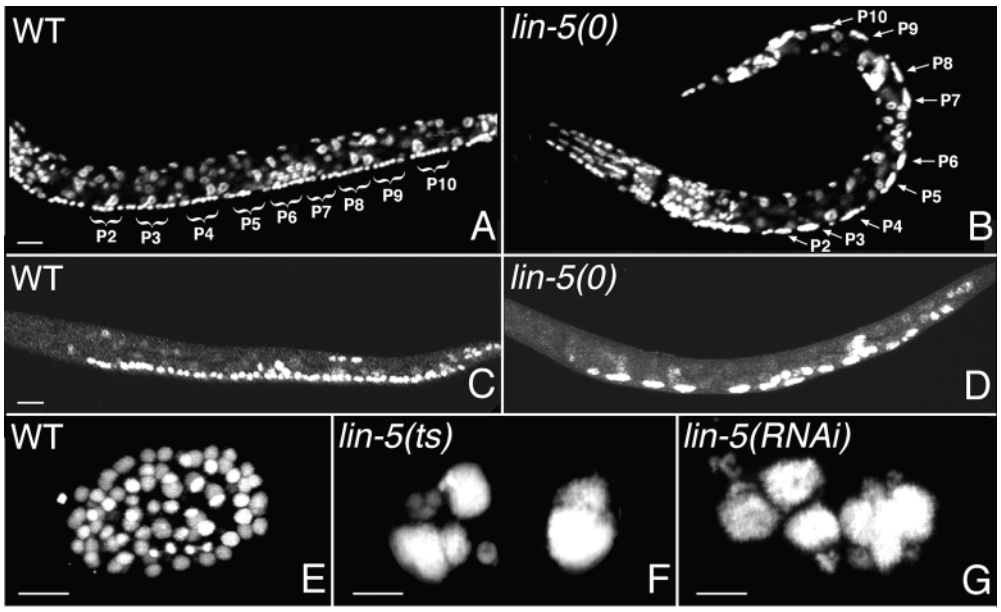

Figure 1. lin-5 mutants are defective in mitosis, but continue DNA replication. A and B, Early L2 stage wild-type animal (A) and *lin-5(e1348)* mutant (B) fixed and stained with the DNA dye PI. Anterior is to the left, ventral is down. In the *lin-5* mutant, the ventral cord P cells are undivided and polyploid, whereas in the wild-type animal, the corresponding cells have divided multiple times. The P cells and daughter cells are indicated for P_2–P_{10}. Between the P cells are neuronal nuclei that do not divide postembryonically and have 2n DNA contents. C and D, Wild-type animal (C) and *lin-5(e1348)* mutant (D) stained after labeling with BrdU from 6–14 h of development. DNA synthesis appeared normal in *lin-5* mutants, but was not followed by cell division. Incorporation of BrdU can be detected in all P cells and several other postembryonic blast cells. E–G, Single embryos: wild-type embryo (E), *lin-5(ev571*ts*)* embryo developed at the nonpermissive temperature (F), and *lin-5(RNAi)* embryo (G) stained with PI to illustrate the early embryonic arrest with polyploid nuclei in the absence of maternal *lin-5* function. Bars, 10 μm.

ilar numbers of ventral cord P cells with phosphorylated histone H3 (Fig. 2). Thus, in agreement with the morphological changes, the periodic activation and inactivation of NCC-1(Cdk1) appeared to continue in *lin-5* mutants.

After abortive mitoses, *lin-5* mutants continued subsequent rounds of DNA replication. As a result, the blast cells that normally generate the postembryonic lineages became large and polyploid, as was visualized by DNA staining with PI, as well as labeling with the thymidine analogue BrdU, followed by immunostaining (Fig. 1, A–D). The number of abortive divisions for each cell and the polyploidy of its DNA reflect the number of divisions in the lineage (Albertson et al., 1978; and data not shown). Despite the lack of cell division, *lin-5* mutants grow substantially and develop into adults that are sterile, uncoordinated, and contain essentially the number of cells of newly hatched larvae (Albertson et al., 1978; Sulston and Horvitz, 1981).

We addressed the role of *lin-5* during embryonic cell divisions by using a temperature-sensitive (ts) mutation. The conditional allele *lin-5(ev571*ts*)* conferred a recessive loss-of-function phenotype that became stronger with increases in temperature (data not shown). Shifting the temperature from 15 to 25°C at any time of embryonic or postembryonic development caused *lin-5(ev571*ts*)* mutants to fail subsequent cell divisions, but not DNA replication (Fig. 1 F; and data not shown). Inhibition of *lin-5* function by RNA-mediated interference (RNAi) also resulted in early embryonic arrest (Fig. 1 G). We conclude that *lin-5* is required for mitotic divisions during embryonic, as well as larval, development and that maternally provided wild-type product is sufficient for embryogenesis.

lin-5 Mutants Exit Mitosis without Chromosome Segregation

As described above, mitoses become defective even before chromosome alignment at the metaphase plate in *lin-5(0)* mutants (Fig. 2). Based on studies of other eukaryotes, such defects might be expected to trigger surveillance mechanisms that delay exit from mitosis and initiation of the next S phase (for review, Skibbens and Hieter, 1998). We carefully determined the time in mitosis for P cells, P1–P12, of the ventral nerve cord in wild-type and *lin-5* mutant L1 larvae. The P cells initiate their postembryonic lineages about half-way through the first larval stage. Only the first defective divisions were examined to avoid scoring secondary effects. The time between entry into and exit from mitosis was very similar for the P cells in wild-type and *lin-5(e1348)* animals, confirming the lack of mitotic arrest in *lin-5(0)* mutants (Fig. 3). However, partial loss-of-*lin-5* function appeared to cause a delay. When *lin-5(ev571*ts*)* early L1 larvae were shifted from 15 to 25°C, a few P cells (12/105) completed division. If shifted to 23°C, a slightly higher number of P cells (22/105) divided. These data are in agreement with the incomplete loss-of-function and temperature-sensitive nature of the *lin-5(ev571*ts*)* allele. The duration of defective mitoses at 25°C was slightly longer in *ev571*ts mutants as compared with *lin-5(e1348)* mutants (Fig. 3, average time in mitosis ~24 and 19 min, respectively). Interestingly, P cells in *lin-5(ev571*ts*)* mutants remained in mitosis for significantly prolonged times at 23°C (Fig. 3, average time in mitosis 52 min). Thus, incomplete inactivation of *lin-5* resulted in delayed exit from mitosis, whereas complete inactivation did not. These observations may reflect a role for *lin-5* in preventing prema-

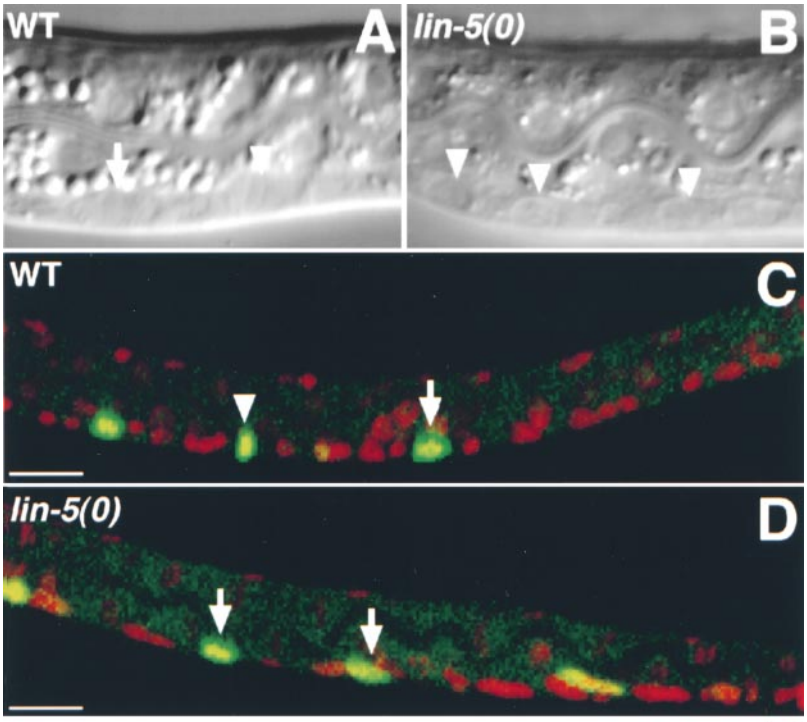

E

Quantitation of mitotic phases

Phenotype	Not Aligned	Metaphase	Anaphase/ Telophase	Phosphorylated H3 (# cells/animal)
WT	57% (291)	27% (138)	16% (80)	2.4± 1.1
lin-5(0)	98% (171)	1% (2)	1% (1)	2.5± 1.1

Figure 2. In *lin-5* mutants, cells enter mitosis, chromosomes condense, but fail to align at the metaphase plate, and periodic activation and inactivation of Cdk1/NCC-1 continues. Synchronously growing L1 larvae were examined during the first round of (attempted) divisions of the ventral cord P cells. A and B, Nomarski microscopy images of living animals showing mitotic P cells at 9 h of postembryonic development. C and D, Epifluorescence images of animals of the same stage, but fixed and stained to visualize phosphorylated histone H3 (green) as a reporter of Cdk1/NCC-1 kinase activity, and counterstained with PI to reveal DNA (red). A, A wild-type animal in which three mitotic P cells are visible, one of which is in metaphase (arrowhead indicates metaphase plate) and one in early anaphase (arrow). B, A *lin-5(0)* mutant, showing three P cells that entered mitosis, but failed to align chromosomes at the metaphase plate. C, Example of a wild-type animal. Three mitotic P cells show phosphorylated histone H3 staining (green), one of which was in metaphase (arrowhead). D, Example of a *lin-5(0)* mutant with mitotic P cells that stained with the phosphorylated histone H3 antibody, but do not show metaphase or anaphase figures. E, Percentages of mitotic P cells with chromosomes that were unaligned, in metaphase alignment, or in anaphase, further demonstrate the lack of alignment and anaphase in *lin-5(0)* mutants. Numbers of P cells counted for each of the mitotic phases are indicated in parentheses. Equal numbers and similarly positioned P cells were found to contain phosphorylated histone H3 in wild-type and *lin-5(0)* mutant larvae, indicating continued activation, as well as inactivation, of NCC-1(Cdk1). Anterior is to the left, ventral is down. WT, Wild-type. Bars, 10 μm.

ture exit from mitosis in addition to its function in promoting chromosome segregation (see Discussion).

The lin-5 Gene Encodes a Novel Protein

To learn more about how *lin-5* functions in cell division, we initiated a molecular analysis. The *lin-5* gene was mapped previously between *lin-26* and *zyg-11* on chromosome II (Fig. 4 A). We identified two overlapping cosmid clones from this region, C03G3 and C30G9, that partially rescued the *lin-5(e1348)* mutant phenotype in germline transformation assays (Materials and Methods). We localized the rescue activity to an 8-kb genomic fragment present on both cosmids (Fig. 4 B). Based on genomic sequences and GENEFINDER predictions available from the *C. elegans* Sequencing Consortium (1998), we created further deletions and identified a single candidate gene. We used genomic DNA from this region to screen two different cDNA libraries, isolated ten clones, and determined the nucleotide sequences of four of these cDNAs. The sequences differed only in their 5′ and 3′ ends, indicating that the clones were independent and derived from identically spliced mRNAs. The longest ORF is predicted to encode a protein of 821 amino acids. This protein is likely the complete LIN-5 protein as the predicted initiator methionine is preceded in the genomic sequence by an in-frame stop codon and no consensus splice acceptor site is present between these stop and start codons. Moreover, Northern blot analysis and reverse transcriptase-PCR experiments confirmed that a single transcript of ~2,650 bp is the major product of this gene (data not shown).

Several experiments confirmed that we indeed had cloned the *lin-5* gene. First, expression of the longest cDNA under the control of heat-shock promoters *hsp16-2* and *hsp16-41* in transgenic lines could partially complement the *lin-5(e1348)* mutation. Specifically, exposure of such embryos to 33°C for one hour resulted in cell divisions in the P cell lineages in a significant percentage of *lin-5* animals. As the P cell lineages were not completely restored, these divisions resulted in formation of abnormal protruding vulva. Animals with protruding vulva were found in three of three transgenic lines expressing the *lin-5* cDNA and not among the progeny from control animals injected with only the dominant marker DNA. Second, in RNA-interference experiments, injection of dsRNA transcribed in vitro from the longest cDNA caused a Lin-5 phenotype in the F1 progeny. All progeny produced eight hours or more after injection were embryonic lethal and

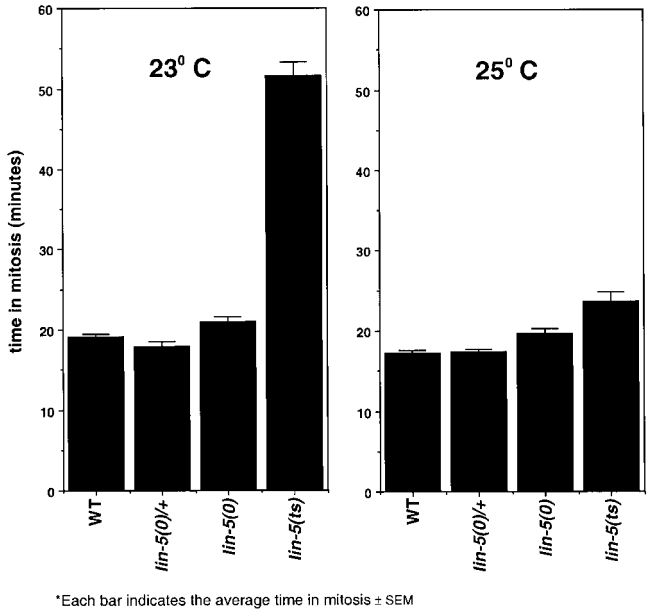

Figure 3. Partial, but not complete, inactivation of *lin-5* delays exit from mitosis, consistent with a *lin-5* function in both mitotic arrest and chromosome segregation. Arrested early L1 animals were shifted from 15 to 23°C (left) or 25°C (right), stimulated to develop synchronously by addition of food, and examined using Nomarski optics. The time in mitosis, determined as the time from disappearance of the nucleolus until reformation of the nuclear envelope, was recorded for the first (abortive) divisions in the P cell lineages. L1 larvae scored were of wild-type (WT), *lin-5(e1348)/+*, *lin-5(e1348)*, or *lin-5(ev571*ts*)* genotype.

closely resembled *lin-5(ev571*ts*)* embryos at the nonpermissive temperature (Fig. 1, F and G; Table I). In addition, some of the early progeny completed embryogenesis after injection, but failed larval cell divisions and resembled *lin-5(0)* mutants. This latter result is consistent with the interpretation that some of the first brood after RNA injection have maternal gene function, but lack zygotic gene activity (Tabara et al., 1998; Boxem et al., 1999). Finally, we identified the molecular lesions associated with the five existing *lin-5* alleles (Fig. 4, C and D). Four of the five alleles contain G–C to A–T transitions, the most common mutation induced by ethyl methanesulfonate (Anderson, 1995). Alleles *n3070* and *e1348* contain amber mutations and *n3066* contains an ochre mutation; these alleles should terminate translation after 52, 159, and 538 amino acids, respectively. The *e1457* allele contains a missense mutation, changing the glycine residue at position 40 to glutamate. The conditional allele *ev571*ts contains a duplication of 9 bp, followed by a T→C transversion, which results in an insertion in-frame of three amino acids within the coiled-coil domain. Thus, the genetic strength of the five *lin-5* alleles is largely in agreement with the lesions identified.

Searches of existing databases revealed that the LIN-5 protein is not closely related to any protein of known function. However, LIN-5 shares 42% amino acid identity with the protein product of F01G10.5, a gene predicted by the *C. elegans* Sequencing Consortium (1998; Fig. 4 D). We were unable to detect phenotypical consequences of F01G10.5 RNA interference, despite targeting two different segments of the gene and injecting wild-type animals as well as *lin-5(ev571*ts*)* mutants at a semipermissive temperature (20°C, data not shown).

A large central region of the LIN-5 protein, from amino acids 210 to 592, was predicted to form an α-helical coiled coil according to the algorithm of Lupas et al. (1991). Many proteins with myosin-type coiled coils were found in homology searches with LIN-5. We did not consider these proteins to be homologous, as the similarities were restricted in all cases to the residues that form the heptad repeats. Both the NH_2 terminus and COOH terminus of LIN-5 contain five serine/threonine residues followed by a proline, seven of which are conserved in the termini of F01G10.5. These residues are potential targets for phosphorylation by Cdk's and MAP kinases, which may regulate *lin-5* function in mitosis.

LIN-5 Protein Colocalizes with Components of the Meiotic and Mitotic Spindle

To better understand the function of *lin-5*, we determined the subcellular localization of its product. Anti–LIN-5 mAbs were generated after immunizations with a COOH-terminal fragment expressed in and purified from *E. coli*. Using these antibodies in immunostaining experiments, we detected distinctly localized staining during both meiosis and mitosis (see below for details). Such staining was not observed when unrelated antibodies were used. In addition, the immunoreactivity completely disappeared after

Table I. lin-5 Mutants Are Defective in Spindle Positioning

Genotype	Embryos	Spindle orientation: Wild-type (AB P1)	Transverse	Reversal	Longitudinal	Abnormal
	n	%	%	%	%	%
Wild-type	27	92.6 (25)	3.7 (1)	0 (0)	3.7 (1)	0 (0)
lin-5(RNAi)	26	34.6 (9)	38.5 (10)	15.4 (4)	7.7 (2)	3.8 (1)
lin-5(ev571) 26°C	26	34.6 (9)	46.2 (12)	3.8 (1)	11.6 (3)	3.8 (1)

Embryos were fixed and stained with antitubulin and PI. The position of the spindle was examined in two-cell embryos with fully condensed chromosomes in P1 (see Rose and Kemphues, 1998; Materials and Methods). The few abnormally positioned spindles observed in wild-type embryos were likely caused by the fixation and staining procedure. The number of embryos scored for each orientation are in parentheses.

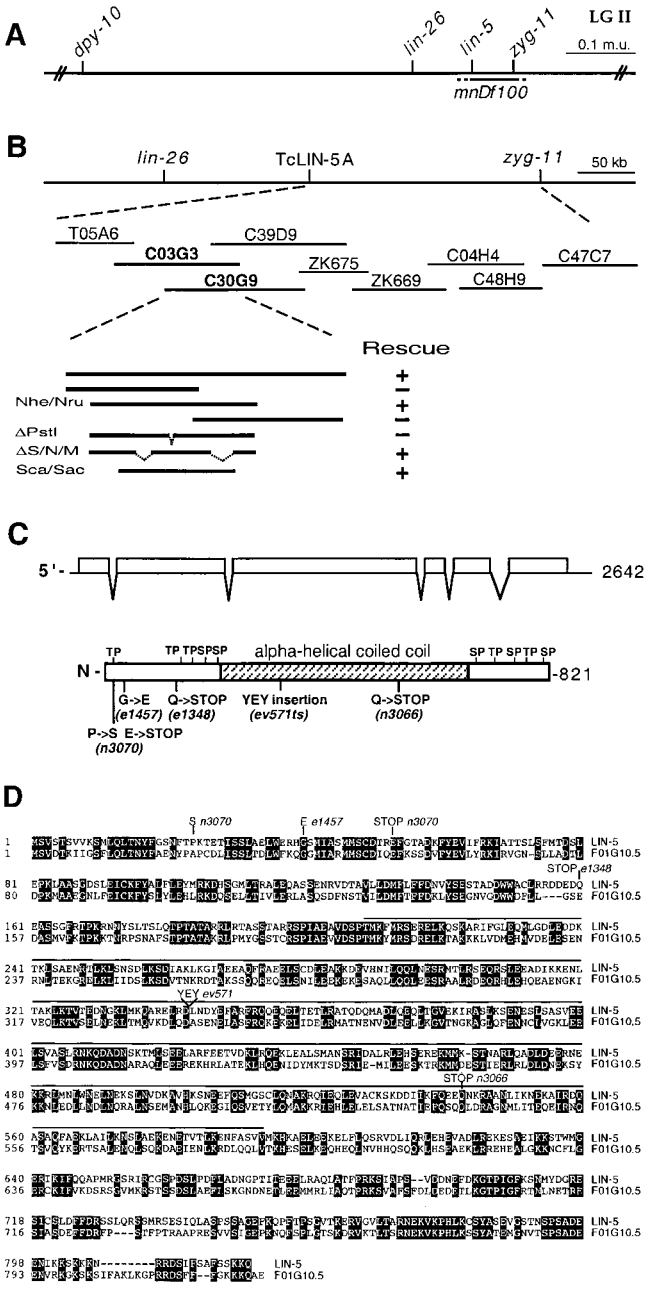

Figure 4. Molecular cloning of the *lin-5* gene. A, Genetic map. The *lin-5* region of linkage group II is indicated, as well as the closest cloned genes to the left and right of *lin-5*. Deletion *mnDf100* includes the *lin-5* gene. B, Physical map and cloning of *lin-5* by germline transformation rescue. Cosmids are shown below the physical map. Overlapping cosmids C03G3 and C30G9 partially rescued the *lin-5(0)* phenotype, as described in Materials and Methods. The minimal rescuing fragment was predicted by the *C. elegans* Sequencing Consortium (1998) to contain three ORFs. Genomic fragments containing the second ORF partially rescued the *lin-5(0)* phenotype. C, The predicted *lin-5* mRNA and LIN-5 protein. The predicted protein contains a large central α-helical coiled-coil domain, as well as ten potential phosphorylation sites for proline-directed kinases, such as Cdc2/Cdk1. D, LIN-5 amino acid sequence and alignment with the *C. elegans* predicted ORF F01G10.5. Black boxes indicate residues of identity. The overlined region indicates the predicted α-helical coiled-coil region shared between LIN-5 and F01G10.5. The molecular lesions in the *lin-5* alleles are indicated below the predicted protein in C and above the *lin-5* sequence in D.

lin-5 RNA interference of control animals. Moreover, in agreement with the genetic strength of the alleles, staining was observed during abortive mitoses in mutant larvae homozygous for the *lin-5(ts)* allele, but not for any one of the four strong *lin-5* mutations. We conclude that these antibodies specifically detect LIN-5.

C. elegans development is initiated by fertilization of oocytes that are in meiotic prophase I. After fertilization, the maternal pronucleus completes meiosis I and II and two polar bodies are expelled. Subsequently, the maternal pronucleus migrates towards the paternal pronucleus in the posterior end of the egg, the two nuclei migrate together to the middle, the nuclear envelopes degrade, and a first mitotic spindle is formed. In immunostaining experiments with anti–LIN-5 antibodies, we observed the following localization pattern: LIN-5 was present at the meiotic spindles in the fertilized egg during meiosis I and II (Figs. 5 A and 6 C). Staining associated with the maternal pronucleus disappeared after completion of meiosis and LIN-5 became localized at the duplicated centrosomes that adjoined the paternal pronucleus (Fig. 5 B). LIN-5 remained localized at the centrosomes until completion of the first mitotic division. In all subsequent mitoses, LIN-5 was associated with the centrosomes and detectable after separation of the centrosomes in prophase until decondensation of chromosomes in telophase (Fig. 5, C–E). LIN-5 was also diffusely present in the cytoplasm and at two other locations; LIN-5 appeared microtubule-associated in cells with metaphase-aligned chromosomes (Figs. 5 F and 6 I). This localization was limited to the region between the poles and did not overlap with DNA staining. Therefore, it appeared to reflect specific association of LIN-5 with kinetochore microtubules. Finally, LIN-5 was diffusely present at the cell cortex in most embryonic cells from the two-cell stage onward (Fig. 5, D–F). During the larval stages, LIN-5 localized to the centrosomes from prophase to telophase and to the cell periphery in late mitosis. In adult hermaphrodites, mitosis is restricted to germ presursor cells in the distal ends of the gonad. LIN-5 was detected at the centrosomes of such cells and, in addition, diffuse cytoplasmic LIN-5 staining was detected in oocytes (data not shown). Finally, strong membrane-associated staining was detected in the gonad at all stages of development (data not shown).

LIN-5 colocalized with several components of the spindle apparatus. Its predominant localization to the centrosomes could reflect association with the centrioles or pericentrosomal matrix or, alternatively, could indicate that LIN-5 associates with microtubules that radiate from the centrosomes. We used the microtubule-destabilizing drug nocodazole to distinguish between these possibilities. Triple-staining experiments were performed to detect DNA, tubulin, and LIN-5 in embryos after nocodazole or control (DMSO) treatment (Fig. 6). Incubation with 20 μg/ml nocodazole for 15 min resulted in elimination of mitotic spindle microtubules in 65% of the embryos (tubulin staining was either absent or restricted to a centrosomal dot in 52 of 80 embryos). Despite the fact that cells were mitotic, as was indicated by DNA condensation, LIN-5 was not localized to the centrosomes in these embryos (Fig. 6). LIN-5 localization to the meiotic spindle also disappeared after nocodazole treatment in 47 of 50 fertilized oocytes (Fig. 6). These results show that LIN-5 is not an

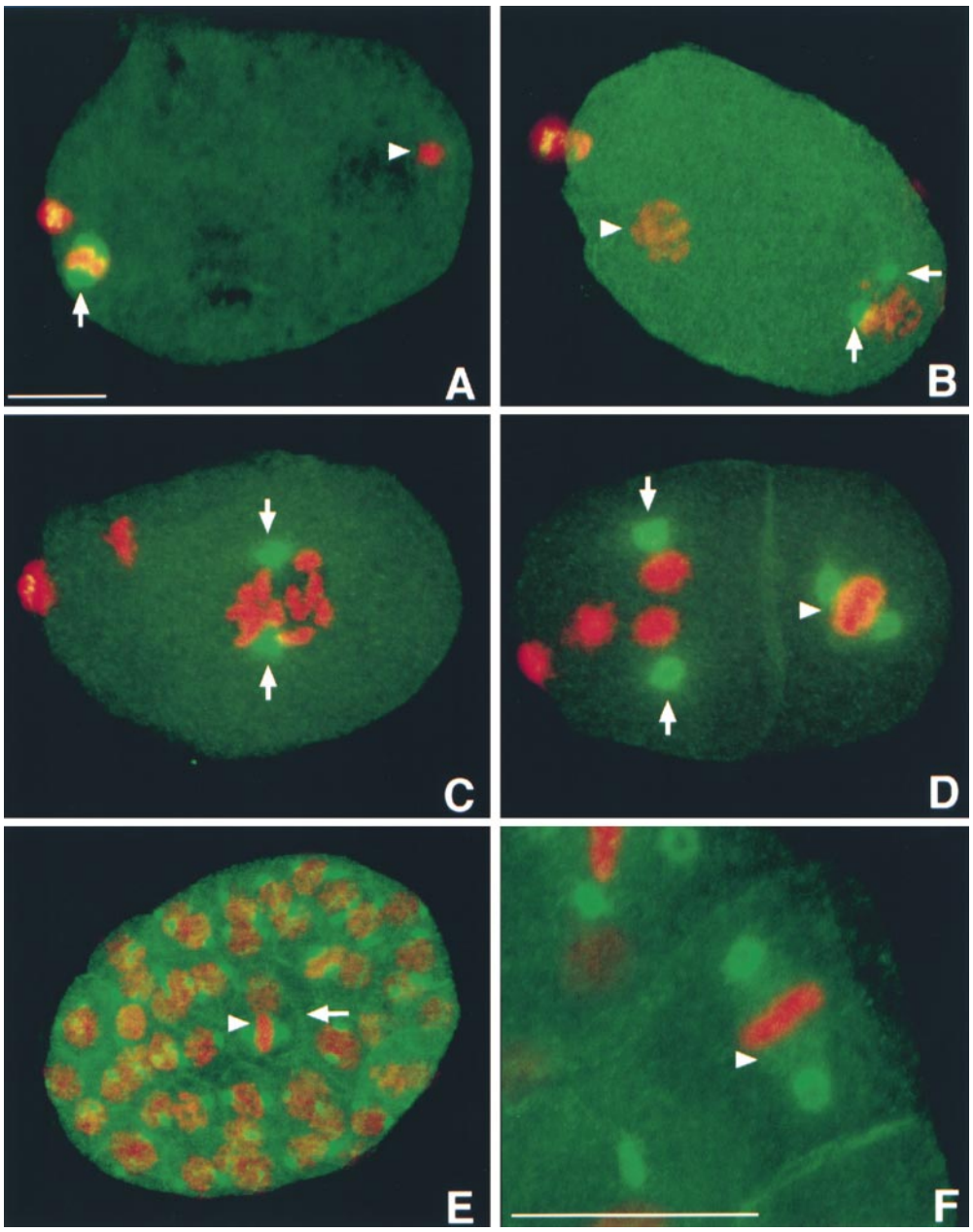

Figure 5. LIN-5 localizes in a cell cycle-dependent manner to the meiotic spindle, mitotic centrosomes, and kinetochore microtubules. In addition, LIN-5 is present in the cytoplasm and at the cell periphery. Staining with LIN-5–specific antibodies is indicated in green, DNA staining with PI in red. A, Fertilized embryo in meiosis II. LIN-5 was localized to the meiotic spindle (arrow). The condensed sperm pronucleus is visible at the posterior of the embryo (arrowhead). Some LIN-5 protein was expelled with the polar bodies that are visible in A–D as large red dots at the anterior (left in all panels) of the embryo. B, One-cell embryo at the time of migration of the maternal pronucleus. LIN-5 was located at the duplicated centrosomes of the decondensed sperm pronucleus (arrows) and was no longer detected at the oocyte pronucleus (arrowhead). C, LIN-5 remained associated with the centrosomes (arrows) during nuclear migration, rotation, and formation of the first mitotic spindle. D, LIN-5 is detected at the centrosomes (arrows) and kinetochore microtubules (arrowhead) of this two-cell embryo. E, LIN-5 is detected at the centrosomes, metaphase spindle (arrowhead), and cell cortex (arrow) of mitotic cells throughout embryogenesis. F, Magnification of a multicellular embryo to illustrate the localization of LIN-5 at the kinetochore microtubules (arrowhead) in metaphase cells. Bars, ~10 μm.

integral component of the centrosome, but rather directly or indirectly associates with the microtubules emanating from the centrosomes.

In conclusion, consistent with its role in chromosome segregation, LIN-5 is localized at the spindle apparatus in meiosis and mitosis. Its localization at the meiotic spindle, mitotic centrosomes, and metaphase microtubules are all dependent on the presence of microtubules.

lin-5 Appears Required for Spindle Force, but Not for Centrosome Duplication or Spindle Assembly

As a component of the mitotic apparatus, LIN-5 could act in spindle assembly and, for instance, be required for centrosome duplication or nucleation of microtubules. Alternatively, LIN-5 could act more specifically in the generation of spindle force and affect either microtubule motor proteins or microtubule dynamics. We examined the spindle apparatus in *lin-5* mutant embryos and larvae to test these possibilities.

Staining with antitubulin antibodies revealed that centrosomes duplicated and migrated to opposite poles in *lin-5(ev571*ts*)* or *lin-5(RNAi)* mutant embryos and *lin-5(0)* L1 larvae. Mitotic microtubules were nucleated, at least in part, and bipolar spindles formed (Fig. 7). In fact, centrosome duplication continued and the number of cen-

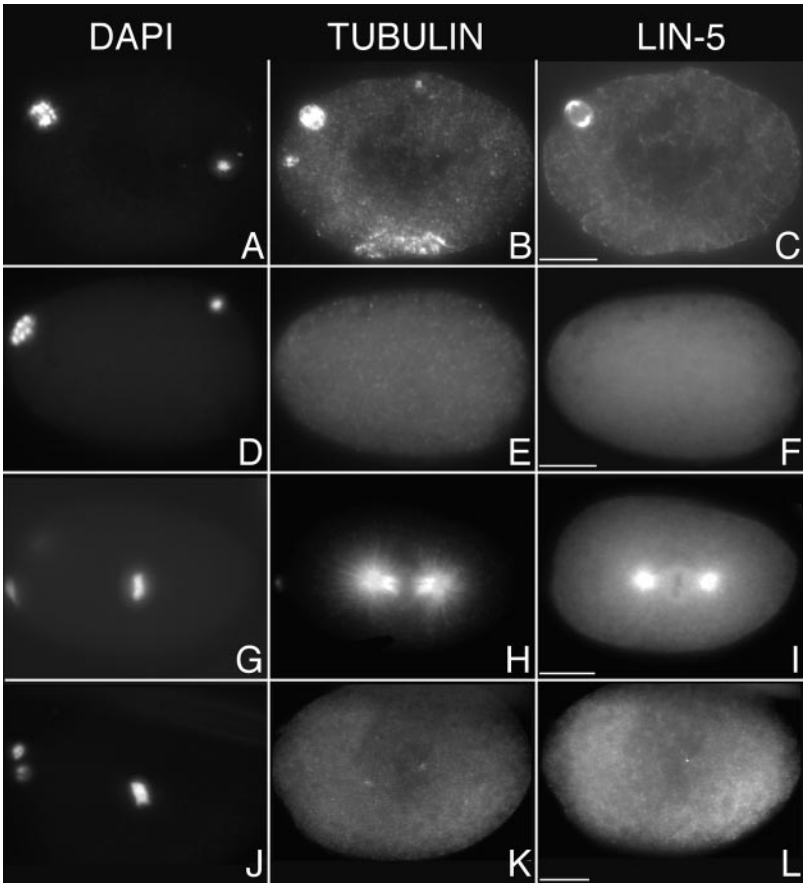

Figure 6. LIN-5 localization is disrupted by treatment with nocodazole. Immunofluorescence micrographs of untreated (A–C and G–I) and nocodazole-treated (D–F and J–L) wild-type embryos stained with DAPI (left), antitubulin antibodies (middle), or anti–LIN-5 antibodies (right) during meiosis (A–F) and mitosis (G–L). In embryos with depolymerized microtubules, LIN-5 did not localize to the meiotic spindle, centrosomes, and metaphase spindle. Anterior is to the left. Bars, ~10 μm.

trosomes doubled with each additional abortive division (Fig. 7 C). Thus, *lin-5* is not required for centrosome duplication. Moreover, DNA replication and centrosome duplication both continued in *lin-5* mutants in the absence of chromosome segregation.

As mentioned above, chromosomes failed to move towards or away from the metaphase plate during abortive mitoses in *lin-5(0)* mutants, indicating absence of spindle force. In addition, we observed defects in rotation of centrosomes and spindle positioning in *lin-5* embryos and L1 larvae. Defects in spindle positioning occurred as early as the first division in *lin-5(RNAi)* and *lin-5(ev571*ts*)* embryos (see below), whereas chromosome congression, segregation, and cytokinesis usually failed after two to four divisions.

The position of the spindle apparatus determines the cleavage plane of the cell, which is an important element in regulating symmetry and direction of cell division, two key aspects of animal development. Centrosome migrations in *C. elegans* have been well studied, in particular during the first two mitotic cleavages (for review, White and Strome, 1996). In wild-type embryos, the first mitotic spindle is oriented along the long axis of the egg (Fig. 8 B). The spindle migrates posteriorly during the first mitosis, causing the first cleavage to produce two unequal cells: a larger anterior cell, AB, and a smaller posterior cell, P1 (Fig. 8 C). After this division, the centrosomes duplicate in both daughters and migrate to opposite poles. In the AB cell, the spindle is formed in this direction and a transverse division follows. In the P1 cell, the spindle rotates 90° and the subsequent division is longitudinal (Fig. 8 D; Table I).

To quantify the defects in spindle positioning and rotation in *lin-5(ts)* and *lin-5(RNAi)* embryos, we stained embryos with antitubulin antibodies and PI. In addition, we followed early embryonic development, using Nomarski optics and time-lapse video recordings, to further characterize the abnormalities. Both methods indicated apparently normal centrosome segregation and spindle formation in early *lin-5* embryos, whereas spindle positioning frequently failed (Figs. 7, D and E, and 8). Deviations from wild-type development were seen as early as meiosis: in 7 of 25 *lin-5(RNAi)* embryos fixed before pronuclear fusion, two maternal pronuclei were formed at the anterior end rather than one (data not shown; and Fig. 8 E). Video recordings of such embryos showed that both maternal pronuclei migrated to the posterior and fused with the paternal pronucleus. The first division appeared symmetrical in 9 of 28 *lin-5(RNAi)* embryos fixed at the two-cell stage (data not shown; and Fig. 8 G). Video microscopy revealed that this defect was caused by failure of the first spindle to migrate posteriorly, after being formed at the correct position. The rocking movements that normally coincide with this migration did not occur during the defective divisions. Embryos in which the spindle was mislocalized nevertheless completed the first cycle of chromosome segregation and cytokinesis. At the two-cell stage, the position of the spindle was examined in embryos with fully condensed chromosomes in P1 (Table I). Approxi-

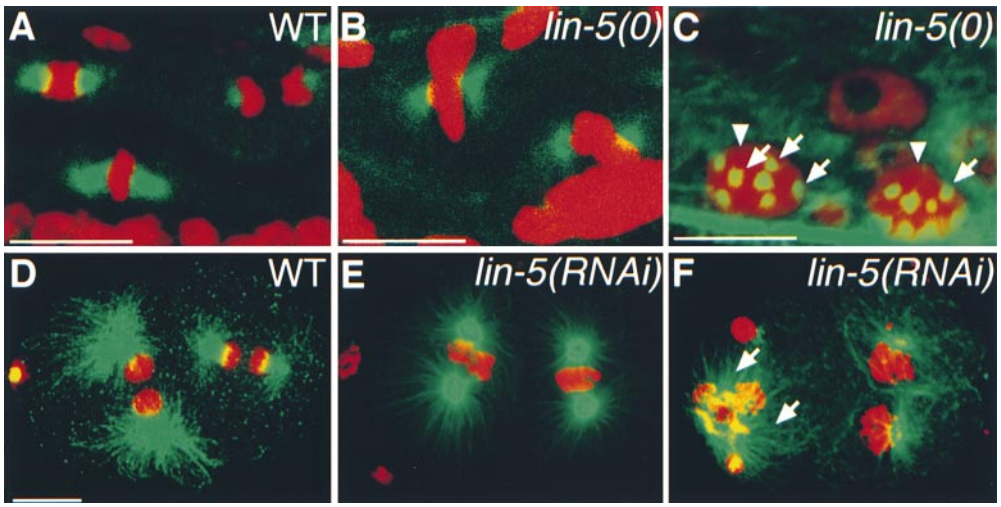

Figure 7. Immunostaining of tubulin, showing that *lin-5* is not essential for bipolar spindle formation, centrosome duplication, and microtubule nucleation, but is required for correct spindle positioning. Tubulin staining is in green, DNA staining in red. Bipolar spindles formed in intestinal nuclei of wild-type (A) and *lin-5* mutant (B) L1 larvae. We also observed apparently normal bipolar spindles in *lin-5* mutants in the Q, V, H, and P cells (data not shown). C, Late L1 *lin-5* mutant with multiple centrosomes (arrows) and polyploid nuclei (arrowheads) in the ventral nerve cord. The number of centrosomes was found to double with each defective division. D, A wild-type embryo showing normal spindle formation and positioning at the two-cell stage. Anterior is to the left. E, A *lin-5(RNAi)* two-cell embryo showing apparently normal spindle formation, but defective spindle rotation. The spindle of the P1 blastomere did not rotate to establish a longitudinal spindle orientation, in contrast to that in the wild-type embryo in D. F, A *lin-5(RNAi)* embryo in which spindle microtubules were formed (arrows), even subsequent to defective nuclear and cytoplasmic division of the AB cell (left). Note that the first rounds of chromosome congression and segregation are completed in *lin-5(RNAi)* embryos, but not in *lin-5(0)* mutant larvae. Bars, ~10 μm.

mately half of the *lin-5* embryos were found to have abnormally positioned spindles. In most of these embryos, the P1 spindle was transverse, indicating failure to rotate to the longitudinal position (Figs. 7 E and 8 H; Table I). Other spindle orientations were also observed with lower frequencies (Table I). These latter defects may have resulted indirectly from a symmetrical first division and coincident defects in the identity of AB and P1. P granules were correctly localized in 39 of 41 embryos that showed no detectable LIN-5 immunoreactivity. These granules segregate to the germline-precursor cells in a microfilament-dependent manner (Strome and Wood, 1983). Thus, the actin cytoskeleton and establishment of cell identities are at least partly functional in *lin-5* embryos after RNAi treatment.

Chromosome movements, centrosome rotation, and spindle migration all are brought about by the spindle apparatus. We conclude that bipolar spindles can be formed in *lin-5* mutants. However, the function of the spindle in generating the forces required for correct chromosome movements and centrosome positioning appear to depend on *lin-5*.

Discussion

lin-5 Is Required Generally for Mitotic Cell Division

In this study, we further defined the function of *lin-5* in vivo, based on observations of the phenotype conferred by null mutations, the conditional *ev571*ts mutation and RNA interference. We cloned *lin-5*, characterized its genomic structure and nucleotide sequences, and identified the molecular lesions in the five existing mutant alleles. In addition, we determined the subcellular localization of the LIN-5 protein during different cell cycle and developmental stages. Finally, we showed that LIN-5 localization to the spindle depends on microtubules. Together, our data establish that *lin-5* encodes a novel component of the spindle apparatus essential for multiple cell division events. We will discuss below how *lin-5* may function.

The presence of maternal product introduces a complication in studying genes that act both early and late in development (see O'Connell et al., 1998; Boxem et al., 1999). Animals homozygous for null mutations in *lin-5* or other essential cell cycle genes have to be obtained from heterozygous parents. The single copy of the wild-type gene in a *lin-5/+* mother provides maternal function and allows embryonic cell division to occur normally. Analysis of the first round of defective postembryonic divisions provides the best information of the null mutant phenotype. However, conclusions based solely on these divisions may be misguided by persistence of maternal product in a subset of cells. In addition, analysis of the null phenotype neither reveals how *lin-5* acts in embryogenesis nor takes advantage of the visibility of mitotic processes in the much larger embryonic cells. By combining experiments with null mutants, a conditional allele, and RNA interference, we have been able to address the function of *lin-5* during various stages of development. These different studies have highlighted different roles. The essential roles of *lin-5* in alignment and segregation of chromosomes, as well as cytokinesis, was most evident during abortive larval divisions in *lin-5(0)* mutants. A role for *lin-5* in spindle positioning was most apparent in early embryonic divisions, although abnormal spindle locations were also detected in *lin-5(0)* larvae stained for tubulin.

Formation of two maternal pronuclei and defective spindle migrations in early *lin-5* embryos implied roles for *lin-5* in meiosis and the first mitotic divisions. Such functions are consistent with the prominent presence of LIN-5 at the meiotic spindle and mitotic centrosomes. However,

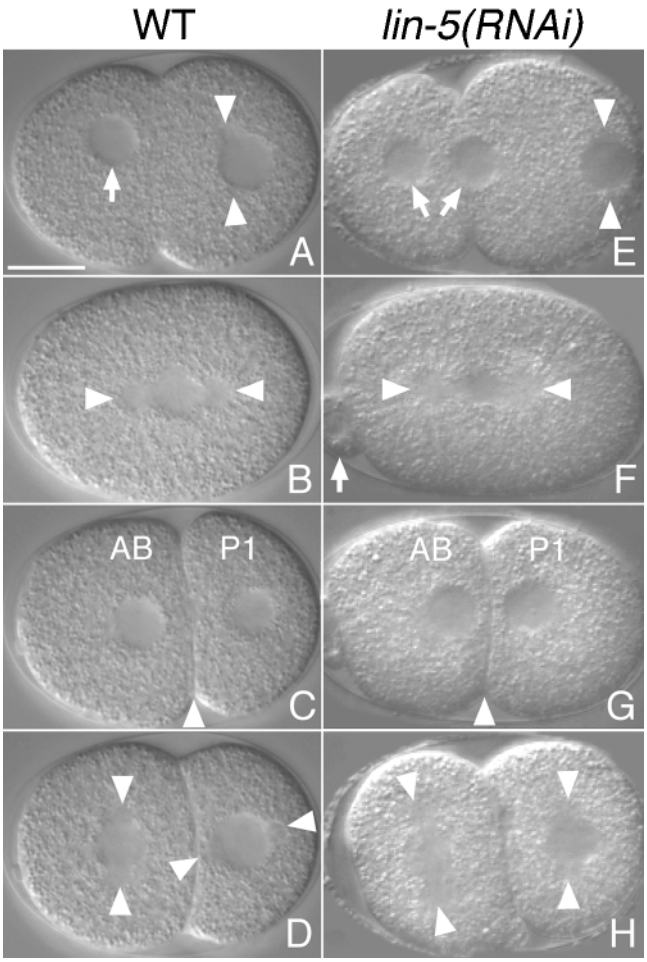

Figure 8. Nomarski images of living embryos. A–D, Selected images from a chronological time-lapse sequence showing early division events in a wild-type embryo. E–H, Images from multiple *lin-5(RNAi)* embryos illustrating defects in meiotic division and mitotic spindle positioning. Anterior is to the left, ventral is down. A and E, Pronuclear migration and pseudocleavage. During meiosis in the wild-type, a single maternal pronucleus is formed (arrow) that migrates to the posterior. Meiotic defects can result in the formation of two maternal pronuclei (arrows) in *lin-5(RNAi)* embryos. Arrowheads indicate the sperm pronucleus with duplicated centrosomes. B and F, Formation of the first mitotic spindle. Asters are indicated by arrowheads; arrow points to an abnormally large polar body in the *lin-5(RNAi)* embryo. C and G, Two-cell embryos. The *lin-5(RNAi)* embryo has divided symmetrically. Arrowheads indicate cleavage plane. D and H, Preceding the second divisions, the centrosome/nucleus complex has rotated in the wild-type P1 blastomere, but not in the *lin-5(RNAi)* embryo. Arrowheads indicate spindle positions. Bar, 10 μm.

a few rounds of chromosome segregation and cytokinesis were generally completed, despite the abnormal spindle positions. It is possible that these first divisions are driven by residual or paternally provided *lin-5* function. However, after RNA interference, LIN-5 protein was no longer detectable at the meiotic spindles, centrosomes, cell periphery, and cytoplasm, indicating a severe and possibly complete loss of protein. LIN-5 was also not detected in spermatozoa, making it unlikely that early divisions depend on paternal wild-type product formed before inactivation of *lin-5*.

As an alternative explanation, intrinsic differences between early and later divisions could determine whether or not *lin-5* is essential for chromosome segregation. A number of genes involved in chromosome segregation have different roles in meiotic versus mitotic divisions (Clark-Maguire and Mains, 1994; Matthews et al., 1998). During female meiosis in *C. elegans*, a barrel-shaped bipolar spindle is formed with very short microtubules (Albertson and Thomson, 1993). The organization of this spindle does not involve centrosomes and presumably occurs in a sequence opposite to that seen in mitosis, with microtubule formation starting at the chromatin rather than the poles (Merdes and Cleveland, 1997). However, early mitotic divisions require spindle function over relatively large distances in rapid order. Thus, chromosome segregation during these divisions would be expected to be highly sensitive to defective spindle components. Therefore, we propose that the limited role of *lin-5* in the first mitotic divisions is due to partial redundancy with another gene, possibly with strict maternal expression. The predicted gene, F01G10.5, was an apparent candidate for acting in this way: it encodes a product with 42% overall amino acid identity and similar in size and structure to LIN-5. However, we were unable to detect any functional overlap between F01G10.5 and *lin-5*. Injection of F01G10.5 dsRNA apparently did not affect the progeny, whether injected alone or together with *lin-5* dsRNA into wild-type animals or partial loss-of-function *lin-5* mutants. As *lin-5(ts)* mutant embryos and *lin-5(RNAi)* embryos displayed a highly similar phenotype, *lin-5* dsRNA most likely interferes specifically with *lin-5* function.

How Does lin-5 Act in Chromosome Segregation?

Based on the loss-of-function phenotype and protein localization data, some predictions can be made about how *lin-5* functions in cell division. Below, we discuss how *lin-5* could act by affecting microtubule dynamics, microtubule/cortex interactions, or the localization/activity of a microtubule motor.

The primary amino acid sequence does not reveal a function, as the only prominent feature of the LIN-5 protein is a central coiled-coil domain. This domain likely is used to form stable associations with either LIN-5 itself or with other proteins (Lupas, 1996). Coiled coils are found in proteins as diverse as transcription factors and keratins, and many coiled-coil proteins have been implicated in spindle function (e.g., Stearns and Winey, 1997). In database searches, we identified a large number of proteins with weak similarity to the coiled-coil domain in LIN-5. However, amino acid identities did not extend beyond the heptad repeats in any protein, with the exception of the product of predicted *C. elegans* gene F01G10.5.

Among the proteins that share similarity with the LIN-5 coiled-coil domain are structural components of the spindle pole bodies and centrosomes. LIN-5 is not an integral constituent of the centrosomes, but rather locates to the microtubules that emanate from the spindle poles. This conclusion is based on a number of observations. First, LIN-5 was associated with the meiotic spindle, which is

formed in the absence of centrosomes (Albertson and Thomson, 1993). Second, LIN-5 was not detected at the centrosomes until after their duplication and separation. Third, LIN-5 was detected at the kinetochore microtubules in metaphase cells. Finally, the localization of LIN-5 at the centrosomes and spindle was disrupted by microtubule depolymerization with nocodazole.

In the absence of *lin-5* function, a bipolar spindle is formed that fails to position itself or to move the chromosomes. Spindle migration and chromosome movements depend on forces generated by a large number of motor proteins in concert with microtubule assembly and disassembly. The meiotic spindles and mitotic apparatus are disorganized and contain abnormally short microtubules in embryos mutant for *zyg-9* (Matthews et al., 1998). ZYG-9 is a *C. elegans* MAP215-related protein and is thought to regulate microtubule turnover (Matthews et al., 1998). Such gross abnormalities in spindle structure were not detected in *lin-5* mutants. In fact, in living *lin-5(RNAi)* embryos, mitotic spindles assembled with normal appearance and timing. Therefore, we do not expect that *lin-5* primarily affects microtubule dynamics, although quantitative studies will be required to further investigate such a role.

Cytoplasmic dynein and at least seven different families of kinesin-related proteins have been found associated with the spindle (for reviews, Hoyt et al., 1997; Stearns, 1997). Several of these motor proteins show M phase-dependent localizations that partly overlap with LIN-5. Perhaps the best match in mutant phenotype and protein localization exists between *lin-5* and cytoplasmic dynein motors. Dynein motors have been implicated in multiple mitotic functions, including nuclear migration, centrosome separation, spindle organization, spindle orientation, and cytokinesis (for reviews, Hoyt et al., 1997; Stearns, 1997; Karki and Holzbaur, 1999). The localization of cytoplasmic dynein is equally diverse and includes the meiotic spindle, mitotic centrosomes, and cell cortex. Dynein is present in the cell in large protein complexes with multiple subunits. Distinct functions of dynein motor complexes likely depend on specific subunits. For instance, a complex that includes NuMA and dynactin has been implicated in mitotic spindle assembly and is located at the centrosomes in mammalian cells (Merdes et al., 1996). Another component, DNC-1/p150^{Glued}, is localized at a cortical microtubule attachment site in early *C. elegans* embryos and acts together with DNC-2/dynamitin in cleavage plane specification (Skop and White, 1998). Importantly, staining of *C. elegans* embryos with antibodies that recognize the dynein heavy chain has shown a partial overlap in subcellular localization with LIN-5 (Gönczy et al., 1999b). Most notable is the observation that both proteins are located at the cell cortex, in addition to the spindle, which has not been described for any member of the family of kinesin-related motor proteins. Based on the similarities in localization, we favor a model in which LIN-5 is required for the localization or regulation of a specific cytoplasmic dynein motor complex.

Cytokinesis Depends on lin-5 Function

Cytokinesis could either directly or indirectly require *lin-5* function. On one hand, a significant percentage of *lin-5* RNAi-treated embryos have multinucleated cells. This observation indicates that cytokinesis can fail despite completion of chromosome segregation, as seen in cytokinesis-specific mutants (Swan et al., 1998; Gönczy et al., 1999a). On the other hand, the failure to undergo cytokinesis is generally preceded by defective chromosome segregation in *lin-5* mutants. In fact, after *lin-5*-RNAi treatment, some early embryos formed extra ectopic division planes and anucleate cells. As the specification of the cleavage plane is dictated by the spindle, *lin-5* might affect cytokinesis through its spindle function. The role of the spindle in cytokinesis likely involves two types of microtubules. The spindle pole position appears to be sensed by the cortex through an interaction with astral microtubules (reviewed by Strome, 1993). This interaction likely determines the position of the actomyosin ring. In addition, microtubules of the spindle midzone have important roles in the completion of cleavage (Wheatley and Wang, 1996). LIN-5 is not detected at the astral microtubules, the midzone microtubules, or the cleavage furrow. Therefore, it is unlikely that LIN-5 actively participates in the cleavage process. The lack of anaphase in *lin-5* mutants should prevent the midzone localization of essential regulators of cytokinesis, such as kinesins and members of the Polo and Aurora kinase families (for review, Field et al., 1999). Thus, cytokinesis could fail as an indirect consequence of LIN-5 absence. However, LIN-5 is present at the spindle, as well as the cell periphery. This localization and the observed roles in polar body formation, spindle rotation, and chromosome movements may all be explained by a requirement for *lin-5* in promoting spindle/cortex contacts that also affect cytokinesis.

lin-5 May Be Required for a Mitotic Checkpoint

In most animals studied, embryonic divisions lack certain cell cycle controls and consist of rapidly alternating S and M phases (for review, Hartwell and Weinert, 1989). *C. elegans* embryos treated with microtubule-interfering drugs continue DNA replication in the absence of chromosome segregation (Laufer et al., 1980; Strome and Wood, 1983), consistent with absence of a spindle assembly checkpoint. Therefore, checkpoint function must be examined during the conventional cell cycles later in development. It is presently unknown when *C. elegans* cell cycles acquire G1 and G2 phases and when a mitotic checkpoint might be established. Based on the time between embryonic divisions (Schierenberg et al., 1980; Sulston et al., 1983), switching to more conventional cycles may be gradual and lineage-dependent. We have been unable to study the spindle checkpoint directly during postembryonic development, as *C. elegans* larvae appeared highly resistant to all tested microtubule-interfering drugs (see Materials and Methods). The *C. elegans* Sequencing Consortium (1998) has identified homologues of several genes that act in the spindle assembly checkpoint in other species, including BUB1, BUB2, and MAD2, suggesting conservation of this checkpoint.

In *lin-5* null mutants, blast cells continued to cycle without chromosome segregation, even during larval development. This observation indicates either that *lin-5* acts in a process not monitored by a mitotic checkpoint or that *lin-5*

is required to engage such a checkpoint. We observed that cells delayed their exit from mitosis after incomplete inactivation of *lin-5*. Together, these observations are consistent with a dual role for *lin-5*. Specifically, *lin-5* might act both to promote chromosome segregation and to prevent premature exit from mitosis in response to defects in chromosome segregation. In this case, complete inactivation of *lin-5* would remove both functions, whereas partial inactivation could have a differential effect, such as preventing chromosome segregation while still allowing a checkpoint-induced delay. Further studies will be required to test this hypothesis.

In summary, we propose that *lin-5* has at least two direct roles in cell division: a role in spindle positioning and a role in chromosome movement. In addition, *lin-5* is involved directly or indirectly in cytokinesis and in the coupling of DNA replication, centrosome duplication, and mitotic division. As outlined above, we favor the model that *lin-5* brings about its functions by localizing or regulating a motor–protein complex and/or by promoting the connection between spindle microtubules and the cell cortex. Further studies of *C. elegans* should help define how *lin-5* acts during cell division and provide further insights into the mechanisms that accomplish accurate chromosome segregation in animal cells.

We express our gratitude to David Merz and Joe Culotti for gift of the *ev571* allele, Ed Harlow and Chidi Ezuma-Ngwu for help with mAbs, Karen Bennett for P-granule antibodies, Alan Coulson and Michel Labouesse for physical map information and cosmids, Beth James for sequencing assistance, and Alex Knight for the MacStripe program. We thank Nick Dyson, Ridgely Fisk, Iswar Hariharan, Anne Hart, and Marc Vidal for critically reading the manuscript. We are grateful to Yimin Ge and the Cutaneous Biology Research Center of the Massachusetts General Hospital for confocal analysis.

The *Caenorhabditis* Genetics Center, supported by the National Institutes of Health National Center for Research Resources, provided several strains for this work. H.R. Horvitz is an Investigator of the Howard Hughes Medical Institute. This work was supported by a fellowship to S. van den Heuvel from the Helen Hay Whitney Foundation and by grants to S. van den Heuvel from the National Institutes of Health, the Jessie B. Cox Charitable Trust and the Medical Foundation; and by the Howard Hughes Medical Institute.

Submitted: 10 September 1999
Revised: 16 November 1999
Accepted: 3 December 1999

References

Albertson, D.G., and J.N. Thomson. 1993. Segregation of holocentric chromosomes at meiosis in the nematode, *Caenorhabditis elegans*. *Chromosome Res.* 1:15–26.

Albertson, D.G., J.E. Sulston, and J.G. White. 1978. Cell cycling and DNA replication in a mutant blocked in cell division in the nematode *Caenorhabditis elegans*. *Dev. Biol.* 63:165–178.

Anderson, P. 1995. Mutagenesis. *Methods Cell Biol.* 48:31–58.

Boxem, M., D.G. Srinivasan, and S. van den Heuvel. 1999. The *Caenorhabditis elegans* gene *ncc-1* encodes a cdc2-related kinase required for M phase in meiotic and mitotic cell divisions, but not for S phase. *Development.* 126: 2227–2239.

Brenner, S. 1974. The genetics of *Caenorhabditis elegans. Genetics.* 77:71–94.

C. elegans Sequencing Consortium. 1998. Genome sequence of the nematode *C. elegans*: a platform for investigating biology. *Science.* 282:2012–2018.

Clark-Maguire, S., and P.E. Mains. 1994. Localization of the *mei-1* gene product of *Caenorhabditis elegans*, a meiotic-specific spindle component. *J. Cell Biol.* 126:199–209.

Desai, A., and T.J. Mitchison. 1997. Microtubule polymerization dynamics. *Annu. Rev. Cell Dev. Biol.* 13:83–117.

Elledge, S.J. 1996. Cell cycle checkpoints: preventing an identity crisis. *Science.* 274:1664–1672.

Field, C., R. Li, and K. Oegema. 1999. Cytokinesis in eukaryotes: a mechanistic comparison. *Curr. Opin. Cell Biol.* 11:68–80.

Fire, A., S.W. Harrison, and D. Dixon. 1990. A modular set of lacZ fusion vectors for studying gene expression in *Caenorhabditis elegans. Gene.* 93:189–198.

Fire, A., S. Xu, M.K. Montgomery, S.A. Kostas, S.E. Driver, and C.C. Mello. 1998. Potent and specific genetic interference by double-stranded RNA in *Caenorhabditis elegans. Nature.* 391:806–811.

Gönczy, P., H. Schnabel, T. Kaletta, A.D. Amores, T. Hyman, and R. Schnabel. 1999a. Dissection of cell division processes in the one cell stage *Caenorhabditis elegans* embryo by mutational analysis. *J. Cell Biol.* 144:927–946.

Gönczy, P., S. Pichler, M. Kirkham, and A.A. Hyman. 1999b. Cytoplasmic dynein is required for distinct aspects of MTOC positioning, including centrosome separation, in the one cell stage *Caenorhabditis elegans* embryo. *J. Cell Biol.* 144:927–946.

Harlow, E., and D. Lane. 1998. Antibodies: A Laboratory Manual. Cold Spring Harbor Laboratory Press, Cold Spring Harbor, New York.

Hartwell, L.H., and T.A. Weinert. 1989. Checkpoints: controls that ensure the order of cell cycle events. *Science.* 246:629–634.

Horvitz, H.R., and J.E. Sulston. 1980. Isolation and genetic characterization of cell-lineage mutants of the nematode *Caenorhabditis elegans. Genetics.* 96: 435–454.

Hoyt, M., A. Hyman, and M. Bahler. 1997. Motor proteins of the eukaryotic cytoskeleton. *Proc. Natl. Acad. Sci. USA.* 94:12747–12748.

Hoyt, M.A., and J.R. Geiser. 1996. Genetic analysis of the mitotic spindle. *Annu. Rev. Genet.* 30:7–33.

Karki, S., and E.L. Holzbaur. 1999. Cytoplasmic dynein and dynactin in cell division and intracellular transport. *Curr. Opin. Cell Biol.* 11:45–53.

Kirby, C., M. Kusch, and K. Kemphues. 1990. Mutations in the par genes of *Caenorhabditis elegans* affect cytoplasmic reorganization during the first cell cycle. *Dev. Biol.* 142:203–215.

Laufer, J.S., P. Bazzicalupo, and W.B. Wood. 1980. Segregation of developmental potential in early embryos of *Caenorhabditis elegans. Cell.* 19:569–577.

Lieb, J.D., M.R. Albrecht, P.T. Chuang, and B.J. Meyer. 1998. MIX-1: an essential component of the *C. elegans* mitotic machinery executes X chromosome dosage compensation. *Cell.* 92:265–277.

Lupas, A. 1996. Coiled coils: new structures and new functions. *Trends Biochem. Sci.* 21:375–382.

Lupas, A., M. Van Dyke, and J. Stock. 1991. Predicting coils from protein sequences. *Science.* 252:1162–1164.

Matthews, L.R., P. Carter, D. Thierry-Mieg, and K. Kemphues. 1998. ZYG-9, A *Caenorhabditis elegans* protein required for microtubule organization and function, is a component of meiotic and mitotic spindle poles. *J. Cell Biol.* 141:1159–1168.

McKim, K.S., and R.S. Hawley. 1995. Chromosomal control of meiotic cell division. *Science.* 270:1595–1601.

Mello, C.C., J.M. Kramer, D. Stinchcomb, and V. Ambros. 1991. Efficient gene transfer in *C. elegans*: extrachromosomal maintenance and integration of transforming sequences. *EMBO* (*Eur. Mol. Biol. Organ.*) *J.* 10:3959–3970.

Mendenhall, M.D., and A.E. Hodge. 1998. Regulation of Cdc28 cyclin-dependent protein kinase activity during the cell cycle of the yeast *Saccharomyces cerevisiae. Microbiol. Mol. Biol. Rev.* 62:1191–1243.

Merdes, A., and D.W. Cleveland. 1997. Pathways of spindle pole formation: different mechanisms; conserved components. *J. Cell Biol.* 138:953–956.

Merdes, A., K. Ramyar, J. Vechio, and D. Cleveland. 1996. A complex of NuMa and cytoplasmic dynein is essential for mitotic spindle assembly. *Cell.* 87:447–458.

Morgan, D.O. 1997. Cyclin-dependent kinases: engines, clocks, and microprocessors. *Annu. Rev. Cell Dev. Biol.* 13:261–291.

Nasmyth, K. 1996. Viewpoint: putting the cell cycle in order. *Science.* 274:1643–1645.

O'Connell, K.F., C.M. Leys, and J.G. White. 1998. A genetic screen for temperature-sensitive cell-division mutants of *Caenorhabditis elegans. Genetics.* 149:1303–1321.

Okkema, P.G., and A. Fire. 1994. The *Caenorhabditis elegans* NK-2 class homeoprotein CEH-22 is involved in combinatorial activation of gene expression in pharyngeal muscle. *Development.* 120:2175–2186.

Riddle, D.L., T. Blumenthal, B.J. Meyer, and J.R. Priess. 1997. *C. elegans* II. Cold Spring Harbor Laboratory Press, Cold Spring Harbor, New York.

Rose, L.S., and K. Kemphues. 1998. The *let-99* gene is required for proper spindle orientation during cleavage of the *C. elegans* embryo. *Development.* 125: 1337–1346.

Sambrook, J., E.F. Fritsch, and T. Maniatis. 1989. Molecular Cloning: A Laboratory Manual, Second Edition. Cold Spring Harbor Laboratory Press, Cold Spring Harbor, New York.

Schierenberg, E., J. Miwa, and G. von Ehrenstein. 1980. Cell lineages and developmental defects of temperature-sensitive embryonic arrest mutants in *Caenorhabditis elegans. Dev. Biol.* 76:141–159.

Skibbens, R.V., and P. Hieter. 1998. Kinetochores and the checkpoint mechanism that monitors for defects in the chromosome segregation machinery. *Annu. Rev. Genet.* 32:307–337.

Skop, A.R., and J.G. White. 1998. The dynactin complex is required for cleavage plane specification in early *Caenorhabditis elegans* embryos. *Curr. Biol.* 8:1110–1116.

Stearns, T. 1997. Motoring to the finish: kinesin and dynein work together to

orient the yeast mitotic spindle. *J. Cell Biol.* 138:957–960.
Stearns, T., and M. Winey. 1997. The cell center at 100. *Cell*. 91:303–309.
Strome, S. 1993. Determination of cleavage planes. *Cell*. 72:3–6.
Strome, S., and W. Wood. 1983. Generation of asymmetry and segregation of germ-line granules in early *C. elegans* embryos. *Cell*. 35:15–25.
Sulston, J.E., and H.R. Horvitz. 1977. Post-embryonic cell lineages of the nematode, *Caenorhabditis elegans. Dev. Biol*. 56:110–156.
Sulston, J.E., and H.R. Horvitz. 1981. Abnormal cell lineages in mutants of the nematode *Caenorhabditis elegans. Dev. Biol*. 82:41–55.
Sulston, J.E., E. Schierenberg, J.G. White, and J.N. Thomson. 1983. The embryonic cell lineage of the nematode *Caenorhabditis elegans. Dev. Biol.* 100:64–119.
Swan, K.A., A.F. Severson, J.C. Carter, P.R. Martin, H. Schnabel, R. Schnabel, and B. Bowerman. 1998. *cyk-1*: a *C. elegans* FH gene required for a late step in embryonic cytokinesis. *J. Cell Sci*. 111:2017–2027.
Tabara, H., A. Grishok, and C.C. Mello. 1998. RNAi in *C. elegans*: soaking in the genome sequence. *Science.* 282:430–431.
Wheatley, S.P., and Y. Wang. 1996. Midzone microtubule bundles are continuously required for cytokinesis in cultured epithelial cells. *J. Cell Biol*. 135: 981–989.
White, J., and S. Strome. 1996. Cleavage plane specification in *C. elegans*: how to divide the spoils. *Cell*. 84:195–198.
Williams, B.D., B. Schrank, C. Huynh, R. Shownkeen, and R.H. Waterston. 1992. A genetic mapping system in *Caenorhabditis elegans* based on polymorphic sequence-tagged sites. *Genetics*. 131:609–624.
Wood, W.B. 1988. The Nematode *Caenorhabditis elegans.* Cold Spring Harbor Laboratory Press, Cold Spring Harbor, New York.